



# First proteomic analyses of the dorsal and ventral parts of the *Sepia officinalis* cuttlebone

Charles Le Pabic, Arul Marie, Benjamin Marie, Aline Percot, Laure Bonnaud-Ponticelli, Pascal Jean Lopez, Gilles Luquet

## ► To cite this version:

Charles Le Pabic, Arul Marie, Benjamin Marie, Aline Percot, Laure Bonnaud-Ponticelli, et al.. First proteomic analyses of the dorsal and ventral parts of the *Sepia officinalis* cuttlebone. *Journal of Proteomics*, 2017, 150, pp.63-73. <10.1016/j.jprot.2016.08.015>. <hal-02557239>

**HAL Id: hal-02557239**

**<https://hal.science/hal-02557239v1>**

Submitted on 28 Apr 2020

**HAL** is a multi-disciplinary open access archive for the deposit and dissemination of scientific research documents, whether they are published or not. The documents may come from teaching and research institutions in France or abroad, or from public or private research centers.

L'archive ouverte pluridisciplinaire **HAL**, est destinée au dépôt et à la diffusion de documents scientifiques de niveau recherche, publiés ou non, émanant des établissements d'enseignement et de recherche français ou étrangers, des laboratoires publics ou privés.



HAL Authorization

**First proteomic analyses of the dorsal and ventral parts of the *Sepia officinalis*  
cuttlebone**

Charles Le Pabic<sup>a,\*</sup>, Arul Marie<sup>b</sup>, Benjamin Marie<sup>b</sup>, Aline Percot<sup>c</sup>, Laure Bonnaud-Ponticelli<sup>a</sup>,  
Pascal Jean Lopez<sup>a</sup>, Gilles Luquet<sup>a,\*</sup>

<sup>a</sup> Unité Biologie des ORganismes et Ecosystèmes Aquatiques (BOREA, UMR 7208), Sorbonne Universités, Muséum National d'Histoire Naturelle, CNRS, Université Pierre et Marie Curie, Université de Caen Normandie, IRD 207, Université des Antilles, CP 26, 43 rue Cuvier 75005 Paris, France.

<sup>b</sup> UMR 7245 MNHN/CNRS Molécules de Communication et Adaptation des Micro-organismes, Sorbonne Universités, Muséum National d'Histoire Naturelle, CP 54, 43 rue Cuvier 75005 Paris, France.

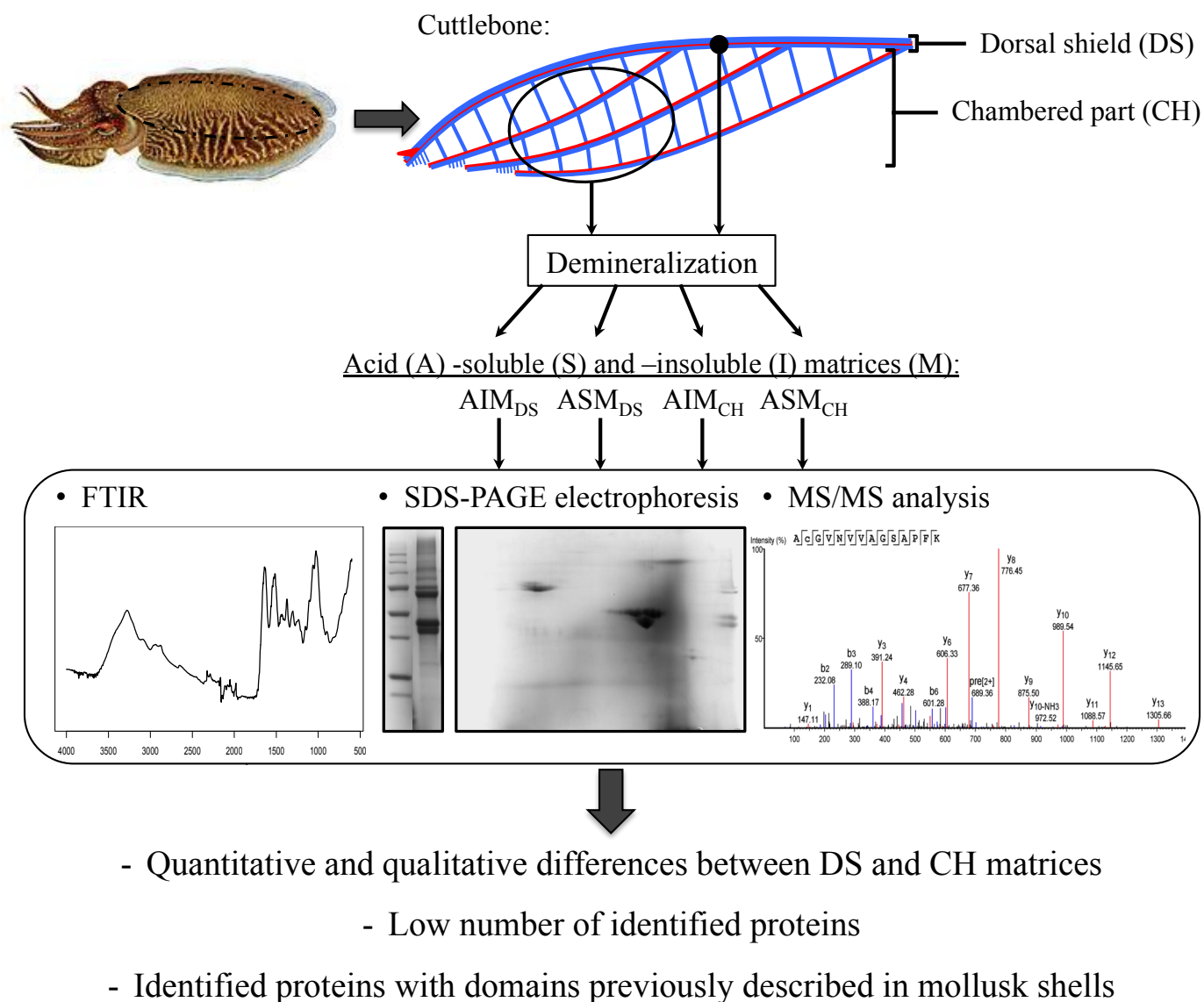
<sup>c</sup> UMR MONARIS, Sorbonne Universités, de la Molécule aux Nano-objets : Réactivité, Interactions et Spectroscopies, UMR 8233 CNRS-Université Pierre et Marie Curie, 75005 Paris, France.

\* Corresponding authors.

E-mail addresses: [clepabic@mnhn.fr](mailto:clepabic@mnhn.fr) (C. Le Pabic); [gluquet@mnhn.fr](mailto:gluquet@mnhn.fr) (G. Luquet)

### *Significance*

The cuttlefish's inner shell, better known under the name "cuttlebone", is a complex mineral structure unique in mollusks and involved in tissue support and buoyancy regulation. Although it combines useful properties as high compressive strength, high porosity and high permeability, knowledge about organic compounds involved in its building remains limited. Moreover, several cuttlebone organic matrix studies reported data very different from each other or from other mollusk shells. Thus, this study provides 1) an overview of the organization of the main mineral structures found in the *S. officinalis* shell, 2) a reliable baseline about its organic composition, and 3) a first descriptive proteomic approach of organic matrices found in the two main parts of this shell. These data will contribute to the general knowledge about mollusk biomineralization as well as in the identification of protein compounds involved in the Sepiidae shell calcification.



**Highlights:**

- First proteomic investigation on organic matrix compounds of a cuttlefish shell.
- Protein composition of DS and CH parts of *S. officinalis* shell appear different.
- Shell organic matrices are globally rich in glycoproteins and low *pI* compounds.
- Most of identified protein compounds contain domains known in biomineralization.
- Our results suggest a transferrin function in the shell DS of *S. officinalis*.

**First proteomic analyses of the dorsal and ventral parts of the *Sepia officinalis*  
cuttlebone**

Charles Le Pabic<sup>a,\*</sup>, Arul Marie<sup>b</sup>, Benjamin Marie<sup>b</sup>, Aline Percot<sup>c</sup>, Laure Bonnaud-Ponticelli<sup>a</sup>,  
Pascal Jean Lopez<sup>a</sup>, Gilles Luquet<sup>a,\*</sup>

<sup>a</sup> Unité Biologie des ORganismes et Ecosystèmes Aquatiques (BOREA, UMR 7208), Sorbonne Universités, Muséum National d'Histoire Naturelle, CNRS, Université Pierre et Marie Curie, Université de Caen Normandie, IRD 207, Université des Antilles, CP 26, 43 rue Cuvier 75005 Paris, France.

<sup>b</sup> UMR 7245 MNHN/CNRS Molécules de Communication et Adaptation des Micro-organismes, Sorbonne Universités, Muséum National d'Histoire Naturelle, CP 54, 43 rue Cuvier 75005 Paris, France.

<sup>c</sup> UMR MONARIS, Sorbonne Universités, de la Molécule aux Nano-objets : Réactivité, Interactions et Spectroscopies, UMR 8233 CNRS-Université Pierre et Marie Curie, 75005 Paris, France.

\* Corresponding authors.

E-mail addresses: [clepabic@mnhn.fr](mailto:clepabic@mnhn.fr) (C. Le Pabic); [gluquet@mnhn.fr](mailto:gluquet@mnhn.fr) (G. Luquet)

## Abstract

Protein compounds constituting mollusk shells are known for their major roles in the biomineralization processes. These last years, a great diversity of shell proteins have been described in bivalves and gastropods allowing a better understanding of the calcification control by organic compounds and given promising applications in biotechnology. Here, we analyzed for the first time the organic matrix of the aragonitic *Sepia officinalis* shell, with an emphasis on protein composition of two different structures: the dorsal shield and the chambered part. Our results highlight an organic matrix mainly composed of polysaccharide, glycoprotein and protein compounds as previously described in other mollusk shells, with quantitative and qualitative differences between the dorsal shield and the chamber part. Proteomic analysis resulted in identification of only a few protein compounds underlining the lack of reference databases for Sepiidae. However, most of them contain domains previously characterized in matrix proteins of aragonitic shell-builder mollusks, suggesting ancient and conserved mechanisms of the aragonite biomineralization processes within mollusks.

## Significance

The cuttlefish's inner shell, better known under the name "cuttlebone", is a complex mineral structure unique in mollusks and involved in tissue support and buoyancy regulation. Although it combines useful properties as high compressive strength, high porosity and high permeability, knowledge about organic compounds involved in its building remains limited. Moreover, several cuttlebone organic matrix studies reported data very different from each other or from other mollusk shells. Thus, this study provides 1) an overview of the organization of the main mineral structures found in the *S. officinalis* shell, 2) a reliable baseline about its organic composition, and 3) a first descriptive proteomic approach of organic matrices found in the two main parts of this shell. These data will contribute to the general knowledge about mollusk biomineralization as well as in the identification of protein compounds involved in the Sepiidae shell calcification.

## Keywords:

Cuttlefish, Biomineralization, Shell, Aragonite, Organic matrix, *Sepia officinalis*, Proteomics

## 1. Introduction

Mollusks are known for their ability to build shells having a huge diversity of sizes, forms and structures. The mollusk shells are mainly composed of calcium carbonate under calcite and/or aragonite polymorphs (rarely vaterite) associated to a small amount of organic compounds (mainly polysaccharides, proteoglycans, glycoproteins and proteins) [1]. Although constituting a very minor fraction of the biomineral, the shell organic matrix is thought to regulate the crystal nucleation, orientation, polymorph, growth and morphology in the calcification process [2]. In order to better understand how organic compounds control calcification and because of their promising applications in biotechnology, shell proteins have been widely studied these last years resulting in the description of a great diversity of protein compounds [e.g. 1,3–10]. However, most of studies describing shell proteins were realized on two groups of mollusks – the bivalves and the gastropods – that share some shell particularities. Indeed, their shells are constituted by the superposition of few calcified layers used for protecting the animal against environmental pressures and predators as well as to support tissue. Moreover, the formation of their shell occurs externally between a thin organic layer (the periostracum) and a calcifying epithelium secreting compounds needed for the shell synthesis [11].

Among other shell-builder mollusks, some Cephalopoda form an original calcified shell constituted by superposed hollow chambers, used to stock gas and thus regulate their buoyancy. Nowadays only three extant cephalopod families conserved this particularity: the Nautilidae, which includes few species with an external coiled shell; the Spirulidae, which contains only 1 species with an inner coiled shell; and the Sepiidae (*i.e.* the cuttlefish), which counts more than 100 species that form an inner straight shell [e.g. 12–14]. This latter structure (also called “cuttlebone”), essentially composed by aragonite, is involved in tissue support and buoyancy regulation as for Spirulidae and Nautilidae, but its morphology and structural organization is quite different. Indeed, Sepiidae shell consists in two distinct regions: the upper side called the dorsal shield and the ventral chambered part (Fig. 1). The dorsal shield is a dense and rigid layer playing an important mechanical role, whereas the chambered part is formed by the superposition of independent hollow chambers of few hundred micrometers height, separated by lamella called septa. Each chamber is open posteriorly allowing the animal to fill them with variable volumes of gas and liquid in order to adjust its buoyancy. Within the chambers, vertical pillars form the supporting elements of the septa. These pillars can be independent or linked together depending on the inner area observed [15–17]. Although both cuttlebone parts associate lamellar and prismatic structures,



their organization differs according to their mineralogy organization and microstructures (Fig. 1). The dorsal shield consists in three layers: the uppermost one is formed of prismatic calcareous tubercles, the central one is characterized by a lamellar organization and the inner one is made by prismatic crystals [16,18]. In the chambered part, each septum consists of a prismatic layer on its lower side, similar as in the pillar, and a lamellar structure on its upper side (previously described as nacre [18,19]) resulting in a septa of around 20  $\mu\text{m}$ -thickness (Fig. 1; for a more detailed description, see [16,17]).

This intricate structure combines contradictory properties as high compressive strength, high porosity and high permeability [20–23], but knowledge about organic compounds involved in its building remains limited. Although the total amount of organic matter – described as being composed of polysaccharides, glycoproteins and proteins – is known to be important in Sepiidae shells (4-10% of the shell dry weight) [22,24–26] in comparison with other mollusks (0.01-5%) [4,7,11]. The main polysaccharide component, the  $\beta$ -chitin, plays a major framework role that allows the set up of the shell [22,24,25,27,28] in association with protein compounds, proposed as organic precursors of the mineralization [29]. Most of the organic compounds involved in this process are synthesized by a monolayered epithelium that surrounds the shell – named “shell sac”, described as a complex tissue composed by 3 to 5 different cell-types [15,16,20,30,31] (Fig. 1). This particularity represents a major difference with other shell-builder mollusks studied thus far.

Despite the importance of proteins in the mollusk shells formation, no detailed protein description has been published yet for Sepiidae shells. Moreover, although obviously distinct and in direct contact with different shell sac tissues (Fig. 1) [16,31], the dorsal shield and the chambered part have been rarely compared (most of studies focusing on the chambered part). In this paper, we analyzed for the first time the shell protein composition of one of the better-known cuttlefish model, the species *Sepia officinalis*. In addition, both shell parts described hereabove have been discriminated.

## **2. Material & Methods**

### *2.1. Shell material and matrix extraction*

The cuttlebones from eight adult *S. officinalis* that were used in this study were obtained from freshly fished specimens along the English Channel coastline. After cuttlebone removing, the superficial organic contaminants were eliminated by 24 h incubation in a 0.25% NaClO solution under constant agitation, and thoroughly rinsed with Milli-Q water. Thereafter, cuttlebones were air-dried at room temperature for 24 h.

In order to investigate the total protein composition of the cuttlebone, an entire cuttlebone (*i.e.* without separation of the dorsal shield and the ventral chambered part) was weighted, grounded into fine powder and demineralized in cold 10% acetic acid for 24 h at 4°C. The solution was then centrifuged at 4°C, 30 min at 1700 g. The supernatant containing the acetic acid-soluble organic matrix (ASM) was filtered and concentrated with an Amicon ultrafiltration system on a Millipore® membrane (Ultracell®; 5-kDa cut-off). After extent dialyses against Milli-Q water (at least 8 times), the ASM solution devoid of acetic acid, was freeze-dried and kept at 4°C until used. The pellet, corresponding to the acetic acid-insoluble matrix (AIM), was rinsed 10 times with Milli-Q water, freeze-dried, weighed and stored at 4°C. These two fractions were kept for direct MS analysis.

To perform a comparative analysis of the protein content of the two main parts of cuttlebone, we carefully separated the dorsal shield from the chambered part. Both parts were then respectively weighed, grounded into fine powder and treated as described above to obtain the AIM and ASM organic fractions from the two structurally different parts. Thus, each shell sample gave 4 fractions, *i.e.* the dorsal shield AIM and ASM (respectively AIM<sub>DS</sub> and ASM<sub>DS</sub>) and the chambered part AIM and ASM (respectively AIM<sub>CH</sub> and ASM<sub>CH</sub>).

## 2.2. Fourier transform infrared (FTIR) spectrometry analysis

ATR-FTIR spectra were recorded using a Bruker Equinox 55 spectrometer equipped with an ATR diamond crystal accessory (Golden Gate®, Specac) and purged with dried air. The diamond is cut to obtain a single reflexion at the crystal/sample interface with an accessible area of 50 µm × 2 mm. A Peltier-cooled DTGS Mid-IR detector, a Mid-IR source and an extended KBr beamsplitter were used. An atmospheric compensation was applied with Opus 6.5 software in order to remove residual H<sub>2</sub>O/CO<sub>2</sub> vapor signal. A background was collected before each sample's spectra. For each lyophilized samples (*i.e.* AIM<sub>DS</sub>, ASM<sub>DS</sub>, AIM<sub>CH</sub> and ASM<sub>CH</sub>), 32 scans were accumulated between 4,000 and 600 cm<sup>-1</sup> with a 4 cm<sup>-1</sup> resolution.

## 2.3. Protein matrix analysis on 1-D gels

The separation of matrix components of the AIM and ASM fractions were performed under denaturing conditions by 1-D SDS-PAGE in 12% polyacrylamide gels (Mini-PROTEAN TGX; Bio-Rad; Hercules, CA, USA). Samples were individually suspended in Laemmli sample buffer (Bio-Rad; Hercules, CA, USA) containing 5% β-mercaptoethanol, heat denatured at 95 °C for 5 min [32], centrifuged for 1 min and kept at 4°C until gel

loading. After preliminary trials, the optimal amounts of organic matrix for gel electrophoresis separation were found to be 100 µg for ASM<sub>CH</sub>, 200 µg for ASM<sub>DS</sub> and 300 µg for both AIM fractions. Because the AIM fractions were only partly solubilized by the buffer, the supernatants collected were called Laemmli-soluble AIM (*i.e.* LS-AIM<sub>DS</sub> and LS-AIM<sub>CH</sub>).

Gel separated proteins were visualized with CBB (Bio-Safe™, Bio-Rad; Hercules, CA, USA) or silver nitrate according to Morrissey [33]. In addition, glycosylations were studied qualitatively on gels, and saccharide moieties were detected by the Periodic Acid Schiff (PAS; Pierce™ Glycoprotein Staining kit; Fisher Scientific, Illkirch, France) and Alcian blue stainings. At pH 2.5, the Alcian blue staining highlights saccharide moieties of glycosaminoglycans carrying polyanionic groups such as carboxyl and sulfate groups, whereas at pH 1, only sulfated compounds were stained [34,35].

#### 2.4. Protein assay and matrix analysis on 2-D gels

In order to estimate the amount of proteins solubilized by the rehydration buffer (urea 8 M, CHAPS 2%, DTT 50 mM, Bio-Lyte® 3/10 ampholytes 0.2% (w/v)) used in the ReadyPrep™ 2-D Starter kit (Bio-Rad; Hercules, CA, USA), the protocol for microtiter plates described in the Bio-Rad protein assay kit II was employed. To avoid possible interferences due to the high urea concentration of the rehydration buffer (that must be kept below 6 M, according to manufacturer protocol), all samples and protein standards were diluted to maintain the rehydration buffer/Milli-Q water ratio constant (1/1; v/v). The protein concentrations were measured at 595 nm on the supernatant of the different fractions after 1 min centrifugation using as standard a bovine serum albumin standard curve (50-350 µg mL<sup>-1</sup> of Milli-Q water).

The four fractions were respectively separated on a 2-D gel PROTEAN® IEF cell (Bio-Rad; Hercules, CA, USA), according to the manufacturer's instructions. AIM<sub>DS</sub> (500 µg organic matrix in 150 µL), ASM<sub>DS</sub> (700 µg in 150 µL), AIM<sub>CH</sub> (1.5 mg in 150 µL) and ASM<sub>CH</sub> (400 µg in 150 µL) were rehydrated in the rehydration buffer and briefly centrifuged to avoid pipetting non-dissolved organic matter. Because the AIM fractions were only partly solubilized by the rehydration buffer, the supernatants collected were called urea-soluble AIM (*i.e.* US-AIM<sub>DS</sub> and US-AIM<sub>CH</sub>). Supernatants were then used to rehydrate overnight strips (7 cm linear, pH 3-10 IPG), and IEF was carried out (250 V for 20 min, 4,000 V for 2 h, followed by 4,000 V until 10,000 Vh). The strips were then transferred for 10 min to equilibration buffer I and II (ReadyPrep™ 2-D Starter kit), rinsed in 1X Tris/Glycine/SDS

buffer (Bio-Rad; Hercules, CA, USA), and positioned on top of precast gradient gels (Mini-PROTEAN TGX, 12% polyacrylamide) covered with 0.5% low melting agarose (w/v) in 1X Tris/Glycine/SDS. Electrophoresis was then performed in standard conditions and the gels were subsequently stained with CBB.

## 2.5. Proteomic analysis of the organic matrix fractions

In order to identify protein compounds present in the dorsal shield and chambered part organic matrices, we separately analyzed the most prominent 1-D gel bands from LS-AIM<sub>DS</sub>, ASM<sub>DS</sub>, LS-AIM<sub>CH</sub> and ASM<sub>CH</sub> using MS. In addition, the total ASM and AIM (*i.e.* without dorsal shield and chambered part split) were directly analyzed by MS (*i.e.* without preliminary protein separation).

### 2.5.1. Band protein digestion and MALDI-TOF/TOF analysis

To remove CBB, excised 1-D gel bands were first unstained by at least 3 baths in a 200  $\mu$ L solution of 25 mM NH<sub>4</sub>HCO<sub>3</sub>, 50% ACN (v/v) for 30 min under stirring. Thereafter, they were subsequently washed in 200  $\mu$ L Milli-Q water and ACN 100%, each time for 15 min under stirring and at room temperature. After supernatant removal, this procedure was repeated a second time. Then, the samples were subsequently reduced with DTT (20 mM, 45 min, 56 °C in 50 mM NH<sub>4</sub>HCO<sub>3</sub> pH 8.1) and alkylated in the dark with iodoacetamide (50 mM, 30 min, at room temperature in 50 mM NH<sub>4</sub>HCO<sub>3</sub> pH 8.1). Excised gel fractions were then rinsed once in 300  $\mu$ L of 25 mM NH<sub>4</sub>HCO<sub>3</sub> pH 8.1, and dehydrated using 300  $\mu$ L ACN 100%. Proteins from dehydrated gel were digested by adding 25  $\mu$ L of trypsin (6  $\mu$ g mL<sup>-1</sup>; Sigma-Aldrich) in 25 mM NH<sub>4</sub>HCO<sub>3</sub> for 15 min at 4 °C. Gel was then completely immersed using 30  $\mu$ L of 25 mM NH<sub>4</sub>HCO<sub>3</sub> solution, and incubated overnight at 37 °C under stirring. Finally, the supernatant was collected and residual peptides contained in gels extracted by subsequent baths of 30  $\mu$ L ACN 50%, formic acid 5% and ACN 100%, pooled with previously collected supernatant. Tryptic peptides were then dried with a SpeedVac<sup>TM</sup> concentrator and stored at -20 °C until MS analysis.

MS experiments were carried out on an AB Sciex 5800 proteomics analyzer equipped with TOF-TOF ion optics and an OptiBeam<sup>TM</sup> on-axis laser irradiation with 1,000 Hz repetition rate. The system was calibrated immediately before analysis with a mixture of Angiotensin I, Angiotensin II, Neurotensin, ACTH clip (1-17), ACTH clip (18-39) and mass precision was better than 50 ppm. Dry sample was re-suspended in 10  $\mu$ L of 0.1% TFA. One  $\mu$ L of this peptide solution was mixed with 10  $\mu$ L of CHCA matrix solution prepared in 50%

ACN, 0.1% TFA. The mixture was spotted on a stainless steel Opti-TOF™ 384 targets; the droplet was allowed to evaporate before introducing the target into the mass spectrometer. All the spectra were acquired in automatic mode employing a typically laser intensity of 3,300 for ionization. MS spectra were acquired in the positive reflector mode by averaging 1,000 single spectra ( $5 \times 200$ ) in the masse range from 700 to 4,000 Da. MS/MS spectra were acquired in the positive MS/MS reflector mode by averaging a maximum of 2,500 single spectra ( $10 \times 250$ ) with a laser intensity of 4,200. For the tandem MS experiments, the acceleration voltage applied was 1 kV and air was used as the collision gas.

### *2.5.2. LC ESI-QTOF MS analysis of whole ASM and AIM*

One mg of total ASM or AIM was reduced with 100  $\mu$ L of 10 mM DTT (Sigma-Aldrich) in 100 mM  $\text{NH}_4\text{HCO}_3$  (Sigma-Aldrich) pH 8.1 for 30 min at 57°C, followed by alkylation with iodoacetamide (50 mM, final concentration; Sigma-Aldrich) for 30 min in the dark and at room temperature. Samples were then freeze-dried. The dry residues were dissolved in 200  $\mu$ L of a 50 mM  $\text{NH}_4\text{HCO}_3$  buffer (pH 8.1) containing 5  $\mu$ g of trypsin (Sigma-Aldrich) and 5% ACN (Sigma-Aldrich), and incubated for 18 h at 37°C. After centrifugation at 14,000 g for 30 min, the supernatants were lyophilized and stored at -20°C until MS analysis.

The peptide digests were re-suspended in 50  $\mu$ L of a solution containing 0.1% trifluoroacetic acid (TFA; Sigma-Aldrich) and 3% ACN. Two  $\mu$ L of the peptide digest from the total organic matrices were separated on a  $\text{C}_{18}$  column ( $150 \times 1$  mm, Phenomenex, France) at a flow rate of 40  $\mu\text{L min}^{-1}$  with 0.1% formic acid (solvent A) and ACN (solvent B), using a gradient that varied from 3 to 50% of B in 45 min. The eluted peptides were analyzed in an ESI-QqTOF mass spectrometer (pulsar i, Applied Biosystems, France), using information dependent acquisition mode. This mode allows switching between MS and MS/MS scans. A 1-s MS scan was followed by two 2-s MS/MS acquisitions using two most intense multiply charged precursor peptide ions (+2 to +4). The fragmented precursor ions were excluded for 60 s in order to avoid reanalysis. Minimum ion intensity for MS/MS experiments was set to 10 counts and collision energy for the peptide ions was determined automatically by the acquisition software.

### *2.5.3. Protein identification and sequence analysis*

Data acquisition and analyses were carried out with Analyst QS software (version 1.1). The mass spectra data were searched against the NCBI non-redundant nucleic acid

databases of the gastropod *Lottia gigantea* (188,590 sequences), the bivalves *Crassostrea gigas* (50,925 sequences), *Elliptio complanata* (138,349 sequences) and *Pinctada fucata* (31,477 sequences), and Cephalopods (360,946 sequences; February 2016), with MASCOT (2.1. version, Matrix Science, London, UK) and PEAKS studio (Canada, version 7.1). *L. gigantea*, *C. gigas*, *E. complanata* and *P. fucata* were chosen as reference shell builder non-cephalopod mollusks because of the quality of their databases, the availability of their genomes (for *L. gigantea* [36], *C. gigas* [37] and *P. fucata* [38]) and their protein description considering the biomineralization process. Cephalopod dataset was represented by 114,034 ESTs and 246,912 nucleotide sequences (ns) mainly originating from *Octopus bimaculoides* (197,284 ns), *S. officinalis* (43,625 ESTs + 512 ns), *Euprymna scolopes* (35,420 ESTs + 5240 ns), *Octopus vulgaris* (32,430 ns) and *Doryteuthis pealeii* (22,033 ESTs + 177 ns). The database search parameters used were: fixed modification = carbamidomethylation, variable modification = deamidation of asparagine and aspartic acid and oxidation of methionine, parent ion mass tolerance = 0.5 Da, fragment ion tolerance = 0.5 Da, missed cleavage = 1, with decoy calculation.

Results from *de novo* sequencing (Peaks studio version 7.5) were filtered by setting average local confidence (ALC) to 80 and residue local confidence to 50%. Only peptides with at least 7 amino acids were considered as reliable sequences. PTM search function of the PEAKS Studio was used to look for unexpected modification in the peptides in order to increase the number of peptide spectral matches. Peptide threshold (denoted as -10lgP) for PEAKS DB was set to 30.

In all cases, the peptide spectral matches were validated only if at least one peptide sequence matched to the translated nucleotide sequence using both Mascot and PEAKS programs, guaranteeing the robustness of the results. Identified nucleotide sequences were translated using the EXPASY translate tool (<http://web.expasy.org/translate/>) and the reading frame and coding sequence were manually validated. The signal peptides and conserved domains were predicted using SMART (<http://smart.embl-heidelberg.de>), and the recognized sequences attempted to be identified using BLASTp analysis performed against UniprotKB database provided by UniProt server (<http://www.uniprot.org/blast/>) using default parameters.

### 3. Results

#### 3.1. Organic matrix extraction and repartition

The results of the extraction reveals an important difference in the amount of organic matter between the two cuttlebone parts studied (*i.e.* dorsal shield and chambered part) with

almost twice more organic matrix in the dorsal shield ( $6.2 \pm 1.5\%$ ; w/w) compare to the chambered part ( $3.4 \pm 0.7\%$ ; w/w). As described for other mollusk shells, most of this extracted matrix corresponds to an insoluble form independently of the part of the cuttlefish shell studied (Table 1).

### 3.2. FTIR profiles of the dorsal shield and chambered part AIMs and ASMs

The global FTIR spectra of organic insoluble and soluble fractions extracted from the dorsal shield and the chambered part of *S. officinalis* shell exhibit typical protein and polysaccharide absorption bands (Fig. 2; Table 2). Nevertheless, the AIM and ASM shell spectra appear to be different. Indeed, whereas the characteristic bands commonly associated with proteins (*i.e.* amide A, I, II and III) are clearly visible in the four spectra, the bands associated with carbohydrate compounds (between  $950\text{--}1,200\text{ cm}^{-1}$ ), appear stronger in the AIM ones (Fig. 2, Table 2). Also, note that the absorption band at  $1,375\text{ cm}^{-1}$ , which is more intense in the AIMs, could be attributed to chitin groups (CH bending,  $\text{CH}_3$  symmetric deformation [39,40]).

In the insoluble fractions, the  $\text{AIM}_{\text{CH}}$  spectrum exhibits a stronger carbohydrate absorption band compared to the  $\text{AIM}_{\text{DS}}$ , which suggests a more important saccharide fraction in this shell part (Fig. 2A). A slight difference can also be observed in the ASM extracts, where the relative intensity of the band at  $1,030\text{ cm}^{-1}$  (and  $1,375\text{ cm}^{-1}$ ) is higher in the chamber part than in the dorsal shield one.

However, these results have to be confirmed because similar patterns can be obtained for protein and polysaccharide mixtures (e.g. for chitin composed of amide groups and a carbohydrate skeleton or for proteins associated to chitin).

### 3.3. Characterization of matrices by 1-D SDS-PAGE

The four extracted fractions ( $\text{LS-AIM}_{\text{DS}}$ ,  $\text{LS-AIM}_{\text{CH}}$ ,  $\text{ASM}_{\text{DS}}$  and  $\text{ASM}_{\text{CH}}$ ) were analyzed by 1-D SDS-PAGE. Gels were subsequently stained with CBB, silver nitrate, PAS and Alcian blue at pH 2.5 and 1 (Fig. 3 and 4), providing constitutive information on the protein composition of each fraction. The four profiles are found to be composed of various distinct macromolecular elements.

The  $\text{LS-AIM}_{\text{DS}}$  shows 7 main bands migrating at apparent molecular weights around 120, 89, 72, 61, 40 and 38 and below 15 kDa with particular thickness of the bands 61, 40 and 38 kDa (Fig. 3A). Two other minor bands at around 240 and 27 kDa are also visible. It is noteworthy that silver nitrate negatively stained 72- and 61-kDa bands. The pH 1 Alcian blue

staining of the compounds present in the 61-kDa band highlights that these compounds carried sulfated sugars. Unfortunately, our experiments did not allow to determine whether the 72-kDa compounds are also sulfated. Faint staining of 40- and 38-kDa bands with Alcian blue carried out at pH 2.5 suggests that they contain small amount of carboxylated sugars. Faint PAS staining suggests that the polypeptides migrating at 120, 89, 61, 40 and 38 kDa are glycosylated (Fig. 3A).

The LS-AIM<sub>CH</sub> shows 3 main bands migrating at around 117, 61 and 38 kDa. Another faint band can also be distinguished around 45 kDa (Fig. 3B). Silver nitrate reveals a more intense staining of this latter band, allows to distinguish two bands at 38 kDa, one faint band just below the 117-kDa band, and strongly stain compounds migrating above 250 kDa. Periodic Acid Schiff stains all bands observed using CBB, with more intense staining of the 117- and 38-kDa bands. Alcian blue staining performed at pH 2.5 reveals that the compounds with the highest molecular weight of this fraction carried carboxylated groups associated with sugar moieties, whereas no band was revealed with Alcian blue at pH 1 (data not shown).

The ASM<sub>DS</sub> shows 4 bands migrating at around 240, 105, 31, and 18 kDa. Notably, the migration front appears intensively stained by CBB. Also, 3 other faint bands can be distinguished around 42, 38 and 19 kDa (Fig. 4A). The 240-, 105- and 31-kDa bands appear clearly glycosylated. Alcian blue staining, at pH 2.5, suggests that compounds around 240 kDa and at the migration front probably carry carboxylated groups but not sulfated groups because no band was revealed with Alcian blue at pH 1 (data not shown).

The ASM<sub>CH</sub> shows 4 main bands migrating around 105, 38, 27 and below 15 kDa. Two gel areas also appear delimited by 53-45 and 20-17 kDa bands (Fig. 4B). The bands at 38, 27, 20 and 17 kDa, stained by CBB, appear negatively stained by silver nitrate. PAS stains the 105-kDa band and reveals a smear from 45 to 17 kDa with faint staining of bands 38, 27, 20 and 17 kDa and a new band around 35 kDa. No band was revealed using both Alcian blue stainings, whatever the pH, suggesting no carboxylation neither sulfation of sugars carried by ASM<sub>CH</sub> compounds.

The protein band patterns of these four fractions suggest that the protein contents, from a qualitative point of view, are different from each other. Based on their apparent molecular masses and their staining reactivity, only two compounds seem shared by more than one fraction: the bands around 105 and 117-120 kDa with polysaccharide moieties observed respectively in the soluble and insoluble fractions. Of course, it remains possible that several proteoforms with similar apparent molecular mass constitute similar sized bands (e.g. sulfated and non-sulfated 61-kDa bands in LS-AIM<sub>DS</sub> and LS-AIM<sub>CH</sub>, respectively).



358

### 359 3.4. Characterization of matrices by 2-D SDS-PAGE

360 In order to further characterize the proteins and their putative post-translational  
361 modifications, each fraction was analyzed by 2-DE (Fig. 5 and 6). As for 1-D gel, the four  
362 profiles were found to be composed of various distinct macromolecular elements.

363 In the case of AIMs, an extremely limited part of the matrix was dissolved in the  
364 rehydration buffer, especially considering AIM<sub>CH</sub> (Table 3). The US-AIM<sub>DS</sub> matrix is mainly  
365 characterized by 3 protein rich areas: a smear around 61 kDa with an pI around 5 (supporting  
366 the sulfated sugar moiety of this compound previously underlined), a series of spots around  
367 40 kDa with pIs between 7 and 8, and a large spot at 38 kDa just below this latter (Fig. 5A).  
368 These compounds are consistent with the most intense bands observed in 1-D electrophoresis  
369 (Fig. 3A). Other faint compounds are visualized at higher pI (120 kDa smear at pI around 8  
370 and 3 spots at same levels than the 38, 40 and 61 kDa compounds visible on the right).  
371 Although difficult to distinguish, compounds of different pIs (around 5 and 8) seem to be  
372 present in the protein fraction migrating below 15 kDa (Fig. 5A).

373 The US-AIM<sub>CH</sub> matrix is mainly characterized by 2 series of spots respectively around  
374 61 and 38 kDa. The first spreads from pIs 5 to 8, whereas the second is a series of 5 spots  
375 spread between pIs 5 and 6 (Fig. 5B). According to 1-D gel PAS staining, these spot series  
376 could be due to different glycosylation states (Fig. 3B). Nevertheless, this could also be  
377 attributed to the presence of other post-translational modifications such as phosphorylations.

378 The 2-DE of both ASM matrices resulted in greater protein extraction and separation  
379 (Fig. 5). The main compounds observed in the ASM<sub>DS</sub> fraction are a series of 6 acidic  
380 polypeptides (pIs from 4.5 to 6.5) of around 31 kDa. Furthermore, small compounds  
381 intensively stained by CBB near the 1-D migration front (*i.e.* 18 and below 15 kDa), appear  
382 here at a high pI around 9 (Fig. 6A).

383 The ASM<sub>CH</sub> mainly exhibits 2 acidic smears around 27 kDa (pI = 4.5 to 6) and a series  
384 of spots around 17 kDa spread from pIs 4.5 to 8, but mainly located in the acidic area (Fig.  
385 6B). These observations are consistent with the most CBB-stained compounds described  
386 using 1-D gel electrophoresis. Two thin smears are also observed at around 105 and 38 kDa  
387 and mean pIs at around 4 and 6.5, respectively.

388

### 389 3.5. Protein identification and sequence analysis

390 The biochemical characterization performed in this study was complemented by a  
391 proteomic analysis aiming to identify proteins involved in the cuttlebone formation. The

whole ASM and AIM (*i.e.* without dorsal shield and chambered part split) were analyzed by HPLC-ESI-MS/MS, whereas most prominent gel bands were analyzed by MALDI-TOF/TOF (see Fig. 3 and 4). The resulting peptide sequences were used for screening the NCBI nucleic acid databases described in section 2.5.3. by using Mascot search engine, excluding peptides assigned to trypsin and keratin. *De novo* sequencing of whole soluble and insoluble fractions allowed identifying 65 unique peptides of between 7 and 14 amino acids length (Table S1). We observed neither some particular richness in Gly, Ser, Ala or acidic residues (Asp and Glu), nor peptides with repetitive residue blocs classically described in biomineralization proteins [e.g. 7,9,49]. However, almost 10% of these peptides present an over-representation of the Leu/Ile residues in their sequence.

Whereas no significant protein hit was obtained from the *L. gigantea*, *C. gigas*, *E. complanata* and *P. fucata* databases, the NCBI Cephalopod database matched for 5 acid nucleic translated sequences. It is noteworthy that all identified protein sequences provided from the embryonic *S. officinalis* ESTs library [41]. This underlined the low representativeness of shell-builder Cephalopods in the NCBI Cephalopod database (less than 15% of the sequence number), especially considering the most diversified group: the Sepiidae.

Peptides from ASM matched with 4 EST sequences (FO196371, FO182034, FO201581 and FO162285), whereas peptides from AIM matched only one EST sequence (FO198959; Table 4). Among the 29 analyzed gel bands, only peptides from one ASM<sub>DS</sub> band (migrating at around 31 kDa, and also found in the whole ASM) were found to match with the FO196371 EST sequence. Among these 5 recognized EST sequences, 4 encode for protein sequences exhibiting a signal peptide (FO182034, FO201581, FO198959, FO162285) and only one being complete (FO182034). This latter contains a type 2 chitin-binding domain (ChtBD2; SM000494) and presents 42.7% identity with a chitin-binding protein (DgCBP-1) of the squid *Dosidicus gigas* [42]. The protein sequence recognized with the highest score contains 1 transferrin domain (TR\_FER; SM000094) and matches with more than 42% identity with fish serotransferrins [e.g. 40]. The three other sequences contain respectively 1 O-Glycosyl hydrolase (Glyco\_18; SM000636), 1 von Willebrand factor type A (VWA; SM000327) and 3 Kunitz (SM00131) domains. The first one best matches with a *Sepia esculenta* chitinase with 63% identity, the second one, with a *Lottia gigantea* uncharacterized protein (42.2% identity) having a chitin binding GO function [36], and the last one, with various serine protease inhibitors.

#### 4. Discussion

Although the aragonitic shell of the cuttlefish presents intriguing features (*i.e.* inner position, straight form, hollow chambers structuration allowing buoyancy regulation, high strength, porosity and permeability combination), no detailed description of its protein compounds have been published thus far. Yet, a better understanding of the processes regulating the biomineralization of this shell-type could bring new perspectives for applications in biotechnology. In order to understand whether the building of the cuttlefish shell is regulated by the same mechanisms than other mollusks, we described the proteins present in the cuttlefish shell organic matrix distinguishing its two main parts: the dorsal shield and the chambered part.

Firstly, from a quantitative viewpoint, the total amount of organic matter extracted with our protocol ( $4.7 \pm 1.1\%$ ; Table 1) appears consistent with data classically measured in other mollusk shells (0.01-5%) although in the high range [4,7,11]. However, this amount appears half as data reported by Florek et al. [26] in whole *S. officinalis* shell using thermogravimetric analyses (9.8%). This difference could be due to sample characteristics (*i.e.* shell part used and/or origin) or differences in the measurement technique used. Considering the organic matter amounts obtained from the chambered part, our value ( $3.4 \pm 0.7\%$ ) is in agreement with the 3-4.5% previously reported by Jeuniaux [25] and Birchall and Thomas [22] after HCl aragonite dissolution. Finally, we observed a relatively high amount of organic matter in the dorsal shield ( $6.2 \pm 1.5\%$ ) compared to other mollusk shells [4,7,11]. However, in view of this measure, the 30-40% estimated from the same shell part by Birchall and Thomas [22] seems largely overestimated. In the light of these discrepancies and according to the known cuttlebone intraspecific variations [44,45], it appears important to consider a likely variation of the amount of organic matter found in *S. officinalis* shells in function of the animal living environment. In this study, all cuttlebones used came from a low-depth area (*i.e.* the English Channel). Thus, according to 1) the shell plasticity highlighted in some mollusks in function of their environment [46], to 2) the absolute need for cuttlefish to have a shell resistant to ambient pressure [23], as well as to 3) the role of organic matter in the mineral structure hardness/elasticity compromise [47,48], it would be interesting to compare our data with *S. officinalis* populations living in deeper environments (e.g. from the Mediterranean Sea).

The FTIR spectra of the four fractions studied exhibit mainly protein and carbohydrate bands (Fig. 2; Table 2) as previously observed for organic compounds extracted from other aragonitic mollusk shells [e.g. 28,47–49] and cnidarian skeletons [52,53]. Our analyses also

suggest that the insoluble fractions contain more carbohydrates than the soluble ones (Fig. 2). This carbohydrate richness is likely due to  $\beta$ -chitin that is known in cuttlefish shell for its scaffold role and was previously described as the main polysaccharide compounds of Coleoidea shells [26,28,52]. Notably, the AIM<sub>CH</sub> seems to be the fraction with the highest polysaccharide proportion as previously suggested by Okafor [27]. However, such polysaccharide bands could also originate from sugars moieties linked with proteins as evidenced by PAS and Alcian blue gel staining (Fig. 3 and 4).

Although non-exhaustive (*i.e.* because describing only urea-soluble fractions of both AIMs), our quantitative protein assays suggest that ASMs are richer in protein compounds than AIMs with ASM<sub>DS</sub> being the richest soluble fraction (Table 3). Such protein richness of the dorsal shield organic matrix has been previously suggested by several studies interested in the chitin-linked compounds in the *S. officinalis* shell [24,25,27]. In view of our SDS-PAGE data (Fig. 4 and 6), this protein amount is likely due (at least in part) to the high amount of 5-15 kDa polypeptides. Such richness in small protein compounds (< 8 kDa) has been reported in the nacre water-soluble matrix of the black-lip pearl oyster *Pinctada margaritifera* with self-organization and protease inhibition properties [55,56]. Finally, the carboxylate moieties present in these small protein compounds suggest an ability to bind calcium ions (Fig. 4).

As for the diversity of proteins, our results of 1- and 2-D SDS-PAGE electrophoreses underlined the predominance of low *pI* proteins, especially considering ASMs, and a global richness in glycoproteins for the four fractions (Fig. 3 to 6). These properties are consistent with the current literature interested in mollusk biomineralization [e.g. 1,3,5,24,48,49,55,56]. Notably, the only sulfated glycoprotein detected in our study has been found in the AIM<sub>DS</sub> whereas compounds with similar moieties are usually considered soluble (Fig. 3A) [49,51,58]. Moreover, it is noteworthy that the electrophoretic profiles from 20 kDa and below, observed on ASM<sub>DS</sub> 1-D gels (Fig. 4A), seems similar to those from *Nautilus macromphalus* (Cephalopoda) nacre presented by Marie et al. [51]. Although the main acidic compounds from this previous study has not been observed in our 2-DE, the migration profile likenesses suggests the conservation of some organic compounds between Nautilidae nacre and Sepiidae dorsal shield (partly constituted by mineral organized similarly than nacre [18]; Fig. 1). Of course, only the complete identification of these putatively shared proteinaceous compounds could allow to assess the existence and the level of conservation.

Proteomics study carried out on the whole soluble and insoluble shell fractions and on the 29 prominent gel bands resulting from LS-AIM<sub>DS</sub>, LS-AIM<sub>CH</sub>, ASM<sub>DS</sub> and ASM<sub>CH</sub> SDS-PAGE electrophoresis resulted only in the identification of 5 protein compounds from current

nucleotide and protein databases (Table 4). Moreover, the detected peptides only matched with the embryonic *S. officinalis* ESTs library [41]. This low number of matches highlights the lack of reference databases for Sepiidae that are under-represented in the used Cephalopod data set. Nevertheless, among the 5 protein compounds identified here, 4 of them (*i.e.* aside from the transferrin protein) contain domains that were previously characterized in matrix proteins of aragonitic shell-builder bivalve and gastropod mollusks [e.g. 8,9,57] – namely ChtBD2, Glyco\_18, VWA and Kunitz domains – suggesting ancient and conserved mechanisms of the aragonite biomineralization processes within mollusks.

The ChtBD2, Glyco\_18 and VWA domains are known for their role in the interaction between organic shell components such as polysaccharides (mainly chitin) and proteins. The presence of ChtBD2 and Glyco\_18 domains are consistent with the chitin scaffold role previously described in various mollusk shell matrices [1,24,25,60,61]. Their likely respective roles consist in the attachment of mineral precipitating compounds and in the chitin framework modification or in shell repair [9,62]. Moreover, the chitin richness of the *S. officinalis* shell (around 25% of organic matrix is  $\beta$ -chitin [25,27]) and its ubiquitous inner repartition (*i.e.* in the central layer of the dorsal shield, septa, inter-septa zones and pillars [16,26,29]) provide good correspondence with our identification of proteins bearing chitin-interaction domain. Similarly, VWA domain have been previously retrieved in various mollusk shell matrices (especially in the Pif-177 nacre matrix protein [63]) and is believed to contribute to biomineralization processes, as being involved in protein-protein interactions and subsequent formation of matrix protein complexes [e.g. 1,62]. In addition, various serine protease inhibitors containing Kunitz-like domains have been previously identified in shell organic matrix and tissues involved in mollusk shell synthesis with potential role(s) in inner proteases regulation and/or exogenous proteases protection [e.g. 8,9,63,64].

To the best of our knowledge, a transferrin protein has not been described in mollusk shell organic matrix so far. The transferrin family is a group of monomeric glycoproteins defined by conserved residue motifs allowing the reversible binding of ferric ion ( $\text{Fe}^{3+}$ ) synergistically with a carbonate anion [67,68]. It has been firstly described as performing essential iron transportation and delivery functions. More recent studies underlined that transferrins are multifunctional proteins with diverse physiological roles only beginning to be understood [e.g. 66,67]. Nevertheless, the function of some transferrin family members can be related to mineralization processes, as it is the case for the ovotransferrin found in the calcitic eggshell [70] and for a mammalian transferrin with a carbonic anhydrase inhibitor activity [71]. In aragonite biomineralization, a transferrin protein has been identified as a major

component of the fish otolith organic matrix necessary for otolith growth [72,73]. Thus, our finding suggests a transferrin role in *S. officinalis* shell biomineralization, especially in the dorsal shield part. Moreover, this observation is consistent with the relative high amount of iron previously reported in the *S. officinalis* shell (from 24 to 300  $\mu\text{g g}^{-1}$  of shell, making the iron the second most concentrated trace metal in this shell [26,74,75]) and questions about a role of this trace element in such structure. Finally, according to the known synergistic ligation of carbonate anion in transferrin binding site [67,68], it can also be hypothesized that transferrin achieves a carbonate supply function for calcium carbonate crystal formation.

## 5. Conclusion

This study is the first proteomic report on organic matrix compounds of a cuttlefish shell. Moreover, we have separately analyzed the proteins of the dorsal shield and chambered part, the two main parts of the shell, both being aragonitic but with clearly different architectures. The general description of the shell organic matrix highlights a similar composition compared to other previously analyzed mollusk shells, with some quantitative and qualitative differences between the dorsal shield and the chamber part. These differences suggest dissimilar processes of biomineralization between both shell parts, associated with different shell sac cells and secretory materials.

Our proteomic analysis identified protein domains already known to play some roles in biomineralization processes, suggesting an ancient and common origin of aragonitic shell biomineralization within mollusks. However, the number of matched proteins remained limited, highlighting the scarcity of databases considering the shell builder cephalopods (*i.e.* mainly the Sepiidae). In order to overcome this hurdle, the transcriptome of the *S. officinalis* shell sac has been recently sequenced and is under analysis. It will allow to complete the proteomic analysis presented here and to better understand how organic compounds are involved in the setting up of this intricate structure.

## Acknowledgments

This work was financially supported by the Muséum national d'Histoire naturelle ATM funding (ATM "Interactions Minéral-Vivant"). The authors thank all the members of the platform PROTEOGEN of the University of Caen for MALDI-TOF/TOF analysis as well as Dr Christelle Jozet-Alves for cuttlebone supply.

## References

- [1] M. Suzuki, H. Nagasawa, Mollusk shell structures and their formation mechanism, *Can. J. Zool.* 91 (2013) 349–366. doi:DOI 10.1139/cjz-2012-0333.
- [2] H.A. Lowenstam, S. Weiner, On biomineralization, in: Oxford University Press, London (1989) pp. 7–23.
- [3] L. Addadi, S. Weiner, Interactions between acidic proteins and crystals: stereochemical requirements in biomineralization., *Proc. Natl. Acad. Sci. U. S. A.* 82 (1985) 4110–4114. doi:10.1073/pnas.82.12.4110
- [4] J. Keith, S. Stockwell, D. Ball, K. Remillard, D. Kaplan, T. Thannhauser, R. 571 Sherwood, Comparative analysis of macromolecules in mollusc shells, *Comp. Biochem. Physiol. Part B Comp. Biochem.* 105 (1993) 487–496. doi:10.1016/03050491(93)90078-J
- [5] J.C. Marxen, W. Becker, The organic shell matrix of the freshwater snail *Biomphalaria glabrata*, *Comp. Biochem. Physiol. Part B Biochem. & Mol. Biol.* 118 (1997) 23–33. doi:10.1016/S0305-0491(97)00010-2.
- [6] S. Sudo, T. Fujikawa, T. Nagakura, T. Ohkubo, K. Sakaguchi, M. Tanaka, K. Nakashima, T. Takahashi, Structure of mollusc shell framework proteins, *Nature.* 387 (1997) 563–564.
- [7] F. Marin, G. Luquet, B. Marie, D. Medakovic, Molluscan shell proteins: primary structure, origin, and evolution, *Curr. Top. Dev. Biol.* 80 (2008) 209–276. 582 doi:10.1016/S0070-2153(07)80006-8
- [8] K. Mann, E. Edsinger-gonzales, M. Mann, In-depth proteomic analysis of a mollusc shell: acid-soluble and acid-insoluble matrix of the limpet *Lottia gigantea*, *Proteome Sci.* 10 (2012) 1–18
- [9] B. Marie, C. Joubert, A. Tayalé, I. Zanella-Cléon, C. Belliard, D. Piquemal, N. Cochenne-Laureau, F. Marin, Y. Gueguen, C. Montagnani, Different secretory repertoires control the biomineralization processes of prism and nacre deposition of the pearl oyster shell, *Proc. Natl. Acad. Sci. U.S.A.* 109 (2012) 20986–20991. doi:10.1073/pnas.1210552109/DCSupplemental.[www.pnas.org/cgi/doi/10.1073/pnas.1210552109](http://www.pnas.org/cgi/doi/10.1073/pnas.1210552109).
- [10] F. Marin, B. Marie, S. Ben Hamada, P. Silva, N. Le Roy, S. Wolf, C. Montagnani, C. Joubert, D. Piquemal, D. Saulnier, Y. Gueguen, “Shellome”: proteins involved in mollusc shell biomineralization – diversity, functions, *Recent Adv. Pearl Res.* (2013) 149–166. <http://hal.archives-ouvertes.fr/hal-00793668/>.
- [11] F. Marin, N. Le Roy, B. Marie, The formation and mineralization of mollusk shell, *Front. Biosci. S4* (2012) 1099–1125.
- [12] E.J. Denton, On buoyancy and the lives of modern and fossil cephalopods, *Proc. R. Soc. London. Ser. B.* 185 (1974) 273–299.
- [13] B. Kröger, J. Vinther, D. Fuchs, Cephalopod origin and evolution: A congruent picture

emerging from fossils, development and molecules, *Bioessays*. 33 (2011) 602–613. doi:10.1002/bies.201100001.

[14] A.L. Allcock, A. Lindgren, J.M. Strugnell, The contribution of molecular data to our understanding of cephalopod evolution and systematics: a review, *J. Nat. Hist.* 49 (2015) 1373–1421. doi:10.1080/00222933.2013.825342.

[15] A. Appellöf, Die schalen von *Sepia*, *Spirula* und *Nautilus*. Studien über den bau und das wachsthum, *K. Sven. Vetensk. Akad. Handl.* 25 (1893) 1–106.

[16] K. Bandel, S. von Boletzky, A comparative study of the structure, development and morphological relationships of chambered cephalopod shells, *The Veliger*. 21 (1979) 313–354.

[17] C. Le Pabic, M. Rousseau, L. Bonnaud-Ponticelli, S. von Boletzky, Overview of the shell development of the common cuttlefish *Sepia officinalis* during early-life stages, *Vie Milieu -Life Environ.* 66 (2016) 35–42.

[18] Y. Dauphin, Microstructures des coquilles de céphalopodes II -La seiche (Mollusca, Coleoidea), *Palaeontogr. Abteilung A*. 176 (1981) 35–51.

[19] H. Mutvei, Ultrastructure of the mineral and organic components of molluscan nacreous layers, *Biomineralization*. 2 (1970) 48–72.

[20] E.J. Denton, J.B. Gilpin-Brown, The buoyancy of the cuttlefish, *Sepia officinalis* (L.), *J. Mar. Biol. Assoc. United Kingdom*. 41 (1961) 319–342.

[21] E.J. Denton, J.B. Gilpin-Brown, Floatation mechanisms in modern and fossil cephalopods, *Adv. Mar. Biol.* 11 (1973) 197–268.

[22] J.D. Birchall, N.L. Thomas, On the architecture and function of cuttlefish bone, *J. Mater. Sci.* 18 (1983) 2081–2086.

[23] P.D. Ward, S. von Boletzky, Shell implosion depth and implosion morphologies in three species of *Sepia* (Cephalopoda) from the Mediterranean Sea, *J. Mar. Biol. Assoc. United Kingdom*. 64 (1984) 955–966.

[24] R.H. Hackman, Studies on chitin IV. The occurrence of complexes in which chitin and protein are covalently linked, *Aust. J. Biol. Sci.* 13 (1960) 568–577.

[25] C. Jeuniaux, Chitine et chitinolyse : un chapitre de la biologie moléculaire, Masson ed., Paris, 1963.

[26] M. Florek, E. Fornal, P. Gómez-Romero, E. Zieba, W. Paszkowicz, J. Lekki, J. Nowak, A. Kuczumow, Complementary microstructural and chemical analyses of *Sepia officinalis* endoskeleton, *Mater. Sci. Eng. C*. 29 (2009) 1220–1226. doi:10.1016/j.msec.2008.09.040.

[27] N. Okafor, Isolation of chitin from the shell of the cuttlefish, *Sepia officinalis* L., *Biochim. Biophys. Acta*. 101 (1965) 193–200.

[28] Y. Dauphin, F. Marin, The compositional analysis of recent cephalopod shell carbohydrates by Fourier transform infrared spectrometry and high performance anion exchange-pulsed



amperometric detection, *Experientia*. 51 (1995) 278–283. doi:10.1007/bf01931112.

[29] A.G. Checa, J.H.E. Cartwright, I. Sánchez-Almazo, J.P. Andrade, F. Ruiz-Raya, The cuttlefish *Sepia officinalis* (Sepiidae, Cephalopoda) constructs cuttlebone from a crystal precursor, *Sci. Rep.* 5 (2015) 1–13. doi:10.1038/srep11513.

[30] S. Kawaguti, A. Oda, Electron microscopy on the cuttlebone-producing cells, *Biol. J. Okayama Univ.* 9 (1963) 41–53.

[31] P.E. Spiess, Organogenese des schalendrüsenskomplexes bei einigen coleoiden cephalopoden des mittelmeeeres, *Rev. Suisse Zool.* 79 (1972) 167–226.

[32] U.K. Laemmli, Cleavage of structural proteins during the assembly of the head of bacteriophage T4, *Nature*. 227 (1970) 680–685.

[33] J.H. Morrissey, Silver stain for proteins in polyacrylamide gels: a modified procedure with enhanced uniform sensitivity., *Anal. Biochem.* 117 (1981) 307–310.

[34] R. Lev, S.S. Spicer, Specific staining of sulphate groups with Alcian blue at low pH, *J. Histochem. Cytochem.* 12 (1964) 309.

[35] R.S. Wall, T.J. Gyi, Alcian blue staining of proteoglycans in polyacrylamide gels using the “Critical electrolyte concentration” approach, *Anal. Biochem.* 175 (1988) 298–299. doi:10.1016/0003-2697(88)90392-2.

[36] O. Simakov, F. Marletaz, S.-J. Cho, E. Edsinger-Gonzales, P. Havlak, U. Hellsten, D.H. Kuo, T. Larsson, J. Lv, D. Arendt, R. Savage, K. Osoegawa, P. de Jong, J. Grimwood, J.A. Chapman, H. Shapiro, A. Aerts, R.P. Otiillar, A.Y. Terry, J.L. Boore, I.V. Grigoriev, D.R. Lindberg, E.C. Seaver, D.A. Weisblat, N.H. Putnam, D.S. Rokhsar, Insights into bilaterian evolution from three spiralian genomes, *Nature*. 493 (2013) 526–531. doi:10.1038/nature11696.

[37] G. Zhang, X. Fang, X. Guo, L. Li, R. Luo, F. Xu, P. Yang, L. Zhang, X. Wang, H. Qi, Z. Xiong, H. Que, Y. Xie, P.W. Holland, J. Paps, Y. Zhu, F. Wu, Y. Chen, J. Wang, C. Peng, J. Meng, L. Yang, J. Liu, B. Wen, N. Zhang, Z. Huang, Q. Zhu, Y. Feng, A. Mount, D. Hedgecock, Z. Xu, Y. Liu, T. Domazet-Lošo, Y. Du, X. Sun, S. Zhang, B. Liu, P. Cheng, X. Jiang, J. Li, D. Fan, W. Wang, W. Fu, T. Wang, B. Wang, J. Zhang, Z. Peng, Y. Li, N. Li, J. Wang, M. Chen, Y. He, F. Tan, X. Song, Q. Zheng, R. Huang, H. Yang, X. Du, L. Chen, M. Yang, P.M. Gaffney, S. Wang, L. Luo, Z. She, Y. Ming, W. Huang, S. Zhang, B. Huang, Y. Zhang, T. Qu, P. Ni, G. Miao, J. Wang, Q. Wang, C.E. Steinberg, H. Wang, N. Li, L. Qian, G. Zhang, Y. Li, H. Yang, X. Liu, J. Wang, Y. Yin, J. Wang, The oyster genome reveals stress adaptation and complexity of shell formation, *Nature*. 490 (2012) 49–54. doi:10.1038/nature11413.

[38] T. Takeuchi, R. Koyanagi, F. Gyoja, M. Kanda, K. Hisata, M. Fujie, H. Goto, S. Yamasaki, K. Nagai, Y. Morino, H. Miyamoto, K. Endo, H. Endo, H. Nagasawa, S. Kinoshita, S. Asakawa, S. Watabe, N. Satoh, T. Kawashima, Bivalve-specific gene expansion in the pearl oyster genome: implications of adaptation to a sessile lifestyle, *Zool. Lett.* 2 (2016) 1–13. doi:10.1186/s40851-016-

- [39] I.F. Amaral, P.L. Granja, M.A. Barbosa, Chemical modification of chitosan by phosphorylation: an XPS, FT-IR and SEM study., *J. Biomater. Sci. Polym. Ed.* 16 (2005) 1575–1593. doi:10.1163/156856205774576736.
- [40] D. Biniaś, M. Wyszomirski, W. Biniaś, S. Boryniec, Supramolecular structure of chitin and its derivatives in FTIR spectroscopy studies, *Polish Chitin Soc.* 12 (2007) 95–108.
- [41] Y. Bassaglia, T. Bekel, C. Da, J. Poulain, A. Andouche, S. Navet, L. Bonnaud, ESTs library from embryonic stages reveals tubulin and reflectin diversity in *Sepia officinalis* (Mollusca — Cephalopoda), *Gene*. 498 (2012) 203–211. doi:10.1016/j.gene.2012.01.100.
- [42] Y. Tan, S. Hoon, P.A. Guerette, W. Wei, A. Ghadban, C. Hao, A. Miserez, J.H. Waite, Infiltration of chitin by protein coacervates defines the squid beak mechanical gradient., *Nat. Chem. Biol.* 11 (2015) 488–495. doi:10.1038/nchembio.1833.
- [43] R. Scudiero, F. Trinchella, M. Riggio, E. Parisi, Structure and expression of genes involved in transport and storage of iron in red-blooded and hemoglobin-less antarctic notothenioids, *Gene*. 397 (2007) 1–11. doi:10.1016/j.gene.2007.03.003.
- [44] S. von Boletzky, Effets de la sous-nutrition prolongée sur le développement de la coquille de *Sepia officinalis* L. (Mollusca, Cephalopoda), *Société Zool. Fr.* 99 (1974) 667–673.
- [45] K.M. Sherrard, Cuttlebone morphology limits habitat depth in eleven species of *Sepia* (Cephalopoda: Sepiidae), *Biol. Bull.* 198 (2000) 404–414.
- [46] M. Charrier, A. Marie, D. Guillaume, L. Bédouet, J. Le Lannic, C. Roiland, S. Berland, J.S. Pierre, M. Le Floch, Y. Frenot, M. Lebouvier, Soil calcium availability influences shell ecophenotype formation in the sub-antarctic land snail, *Notodiscus hookeri*, *PLoS One*. 8 (2013) e84527. doi:10.1371/journal.pone.0084527.
- [47] J.D. Currey, The mechanical consequences of variation in the mineral content of bone, *J. Biomech.* 2 (1969) 1–11. doi:10.1016/0021-9290(69)90036-0.
- [48] A.P. Jackson, J.F. V Vincent, R.M. Turner, The mechanical design of nacre, *Proc. R. Soc. London. Ser. B.* 234 (1988) 415–440.
- [49] J.C. Marxen, M. Hammer, T. Gehrke, W. Becker, Carbohydrates of the organic shell matrix and the shell-forming tissue of the snail *Biomphalaria glabrata* (Say), *Biol. Bull.* 194 (1998) 231–240. doi:10.2307/1543052.
- [50] B. Marie, G. Luquet, J.P. Pais De Barros, N. Guichard, S. Morel, G. Alcaraz, L. Bollache, F. Marin, The shell matrix of the freshwater mussel *Unio pictorum* (Paleoheterodonta, Unionoida): Involvement of acidic polysaccharides from glycoproteins in nacre mineralization, *FEBS J.* 274 (2007) 2933–2945. doi:10.1111/j.1742-4658.2007.05825.x.
- [51] B. Marie, F. Marin, A. Marie, L. Bédouet, L. Dubost, G. Alcaraz, C. Milet, G. Luquet, Evolution of nacre: biochemistry and proteomics of the shell organic matrix of the cephalopod

- Nautilus macromphalus*, A Eur. J. Chem. Biol. 10 (2009) 1495–1506. doi:10.1002/cbic.200900009.
- [52] S. Goffredo, P. Vergni, M. Reggi, E. Caroselli, F. Sparla, O. Levy, Z. Dubinsky, G. Falini, The skeletal organic matrix from Mediterranean coral *Balanophyllia europaea* influences calcium carbonate precipitation, PLoS One. 6 (2011) e22338. doi:10.1371/journal.pone.0022338.
- [53] P. Ramos-Silva, J. Kaandorp, F. Herbst, L. Plasseraud, G. Alcaraz, C. Stern, M. Corneillat, N. Guichard, C. Durlet, G. Luquet, F. Marin, The skeleton of the staghorn coral *Acropora millepora*: Molecular and structural characterization, PLoS One. 9 (2014) e97454. doi:10.1371/journal.pone.0097454.
- [54] T. Furuhashi, A. Beran, M. Blazso, Z. Czegeny, C. Schwarzingner, G. Steiner, Pyrolysis GC/MS and IR spectroscopy in chitin analysis of molluscan shells., Biosci. Biotechnol. Biochem. 73 (2009) 1–11. doi:10.1271/bbb.80498.
- [55] L. Bédouet, F. Rusconi, M. Rousseau, D. Duplat, A. Marie, L. Dubost, K. Le Ny, S. Berland, J. Péduzzi, E. Lopez, Identification of low molecular weight molecules as new components of the nacre organic matrix, Comp. Biochem. Physiol. Part B. 144 (2006) 733–743. doi:10.1016/j.cbpb.2006.05.012.
- [56] L. Bédouet, D. Duplat, A. Marie, L. Dubost, S. Berland, M. Rousseau, C. Milet, E. Lopez, Heterogeneity of proteinase inhibitors in the water-soluble organic matrix from the oyster nacre, Mar. Biotechnol. 9 (2007) 437–449. doi:10.1007/s10126-007-7120-y.
- [57] L. Addadi, J. Moradian, E. Shay, N.G. Maroudas, S. Weiner, A chemical model for the cooperation of sulfates and carboxylates in calcite crystal nucleation: Relevance to biomineralization., Proc. Natl. Acad. Sci. U. S. A. 84 (1987) 2732–2736. doi:10.1073/pnas.84.9.2732.
- [58] B. Marie, G. Luquet, L. Bédouet, C. Milet, N. Guichard, D. Medakovic, F. Marin, Nacre calcification in the freshwater mussel *Unio pictorum*: carbonic anhydrase activity and purification of a 95 kDa calcium-binding glycoprotein, ChemBioChem. 9 (2008) 2515–2523. doi:10.1002/cbic.200800159.
- [59] B. Marie, A. Marie, D.J. Jackson, L. Dubost, B.M. Degnan, C. Milet, F. Marin, Proteomic analysis of the organic matrix of the abalone *Haliotis asinina* calcified shell, Proteome Sci. 8 (2010) 1–11.
- [60] H. Ehrlich, Chitin and collagen as universal and alternative templates in biomineralization, 2010. doi:10.1080/00206811003679521.
- [61] W. Peters, Occurrence of chitin in Mollusca, Comp. Biochem. Physiol. -B Biochem. Mol. Biol. 41 (1972) 541–550.
- [62] K. Tanabe, Y. Fukuda, Y. Ohtsuka, New chamber formation in the cuttlefish *Sepia esculenta* Hoyle, Venus. 44 (1985) 55–67.
- [63] M. Suzuki, K. Saruwatari, T. Kogure, Y. Yamamoto, T. Nishimura, T. Kato, H. Nagasawa, An

acidic matrix protein, Pif, is a key macromolecule for nacre formation, *Science*. 325 (2009) 1388–1390. doi:10.1126/science.1173793.

[64] E.P. Chang, J.S. Evans, Pif97, a von Willebrand and peritrophin biomineralization protein, organizes mineral nanoparticles and creates intracrystalline nanochambers, *Biochemistry*. 54 (2015) 5348–5355. doi:10.1021/acs.biochem.5b00842.

[65] L.D. Gardner, D. Mills, A. Wiegand, D. Leavesley, A. Elizur, Spatial analysis of biomineralization associated gene expression from the mantle organ of the pearl oyster *Pinctada maxima*, *BMC Genomics*. 12 (2011) 1–15. doi:10.1186/1471-2164-12-455.

[66] B. Marie, J. Arivalagan, L. Dubost, S. Berland, A. Marie, F. Marin, Unveiling the evolution of bivalve nacre proteins by shell proteomics of Unionoidae, *Key Eng. Mater.* 672 (2015) 158–167. doi:10.4028/www.scientific.net/KEM.672.158.

[67] E.N. Baker, Structure and reactivity of transferrins, *Adv. Inorg. Chem.* 41 (1994) 389–463.

[68] L.A. Lambert, H. Perri, T.J. Meehan, Evolution of duplications in the transferrin family of proteins, *Comp. Biochem. Physiol. -B Biochem. Mol. Biol.* 140 (2005) 11–25. doi:10.1016/j.cbpc.2004.09.012.

[69] A.L. Hughes, R. Friedman, Evolutionary diversification of the vertebrate transferrin multi-gene family, *Immunogenetics*. 66 (2014) 651–661. doi:10.1007/s00251-0140798-x.

[70] J. Gautron, M. Hincke, M. Panheleux, J.M. Garcia-Ruiz, T. Boldicke, Y. Nys, Ovotransferrin is a matrix protein of the hen eggshell membranes and basal calcified layer, *Connect. Tissue Research*. 42 (2001) 255–267.

[71] M.W. Wuebbens, E.D. Roush, C.M. Decastro, C.A. Fierke, Cloning, sequencing, and recombinant expression of the porcine inhibitor of carbonic anhydrase: A novel member of the transferrin family, *Biochemistry*. 36 (1997) 4327–4336. doi:10.1021/bi9627424.

[72] E. Murayama, A. Okuno, T. Ohira, Y. Takagi, H. Nagasawa, Molecular cloning and expression of an otolith matrix protein cDNA from the rainbow trout, *Oncorhynchus mykiss*, *Comp. Biochem. Physiol. Part B Biochem. Mol. Biol.* 126 (2000) 511–520. doi:http://dx.doi.org/10.1016/S0305-0491(00)00223-6.

[73] E. Murayama, P. Herbomel, A. Kawakami, H. Takeda, H. Nagasawa, Otolith matrix proteins OMP-1 and Otolin-1 are necessary for normal otolith growth and their correct anchoring onto the sensory maculae, *Mech. Dev.* 122 (2005) 791–803. doi:10.1016/j.mod.2005.03.002.

[74] P. Miramand, D. Bentley, Concentration and distribution of heavy metals in tissues of two cephalopods, *Eledone cirrhosa* and *Sepia officinalis*, from the French coast of the English Channel, *Mar. Biol.* 114 (1992) 407–414.

[75] P. Miramand, P. Bustamante, D. Bentley, N. Koueta, Variation of heavy metal concentrations (Ag, Cd, Co, Cu, Fe, Pb, V, and Zn) during the life cycle of the common cuttlefish *Sepia officinalis*, *Sci. Total Environ.* 361 (2006) 132–143.

<http://www.sciencedirect.com/science/article/pii/S0048969705007692>.

Tables:

Table 1: Quantification of organic matrix fractions extracted from the different part of the *S. officinalis* shell (*i.e.* whole organic matrix of shell; respective whole organic matrix of dorsal shield (DS) and chambered part (CH); and respective acid-insoluble and acid-soluble organic matrices of dorsal shield and chambered part; mean  $\pm$  SD;  $n = 5$ ).

Shell part	Fraction	Mean organic matrix (%)	
Dorsal shield	AIM	5.8 $\pm$ 1.4	DS: 6.2 $\pm$ 1.5 Whole: 4.7 $\pm$ 1.1
	ASM	0.4 $\pm$ 0.2	
Chambered part	AIM	3.5 $\pm$ 0.7	CH: 3.4 $\pm$ 0.7
	ASM	0.2 $\pm$ 0.1	

Table 2: Position and assignment of the FTIR major bands in the 600-4,000  $\text{cm}^{-1}$  region for polysaccharides, chitin and proteins (vs: very strong, m: medium, w: weak).

Band position ( $\text{cm}^{-1}$ )	Classical polysaccharide	Chitin (+protein?)	Protein	Assignment
950-1,200	vs	vs	w	CC, CO, COC, COH stretching
1,228-1,265			m	Amide III: NH bending and CN stretching
1,310		m		Amide III: $\text{CH}_2$ wagging
1,375		m		CH bending, $\text{CH}_3$ symmetric deformation
1,445			m	$\text{CH}_2$ and $\text{CH}_3$ deformation
1,510-1,550		m	s	Amide II: NH bending coupled to CN stretching
1,600-1,700		m	s	Amide I: CO stretching
2,800-2,950	w	w	w	CH stretching
3,250-3,300		m	m	Amide A: NH stretching
3,550-3,670	m	m	w	OH stretching

Table 3: Protein concentrations ( $\text{mg g}^{-1}$  organic matter; mean  $\pm$  SD;  $n = 5$ ) of the dorsal shield and chambered part acid-insoluble (AIM) and acid-soluble (ASM) matrices of *S. officinalis* shell, extracted in the 2-D kit rehydration buffer (US: urea-soluble).

Shell part	Fraction	Mean protein concentration ( $\text{mg g}^{-1}$ organic matter)
Dorsal shield	US-AIM	$30 \pm 5$
	ASM	$462 \pm 71$
Chambered part	US-AIM	$< 10$
	ASM	$192 \pm 34$



Table 4: Identification of acid-insoluble and acid-soluble matrix proteins of the *S. officinalis* shell by MS/MS analysis

No.	Fraction	GenBank Acc. No.	Peptide sequence	Peptide score* (Mascott / Peaks)	Protein score* (Mascott / Peaks)	Signal peptide / Complete sequence	Theoretical mass / pI	Identified domain
1	ASM / 31 kDa band ASM <sub>DS</sub>	FO196371	CLEETDADVAFVK	93 / 63	209 / 126	No / No	21.8 kDa / 6.4	1 Transferrin (193 aa)
			ADVTVLDGGDIYLAGK	98 / 63				
			HLTFLDNPAK	80 / 48				
			TSGWFPMSVLFPNK	31 / 32				
			HGNNLYYGYSGAAK	- / 31				
2	ASM	FO182034	LFSEATGK	45	117 / 83	Yes / Yes	16.5 kDa / 8.2	1 Chitin-binding type 2 (66 aa)
			LPGPGYLGDIYIDCPYPK	39 / 39				
			CESFEPVSCGSR	- / 47				
3	ASM	FO201581	QVFVTSTINFLR	63 / 48	123 / 81	Yes / No	20.8 kDa / 9.5	1 O-Glycosyl hydrolase (178 aa)
			GSPIEDKENFAELLK	43 / 49				
4	AIM	FO198959	DGTNTDIGINK	69 / 41	69 / 41	Yes / No	19.2 kDa / 9.3	1 von Willebrand factor type A (167 aa)
5	ASM	FO162285	FDICSLDARPGK	34 / 31	62 / 42	Yes / No	16.2 kDa / 6.7	3 BPTI/Kunitz family (54, 54 and 28 aa)

\* maximum score found (independently of the fraction studied)



### Captions to figures:

Figure 1: Schematic representation of the main constituents of the cuttlefish shell in sagittal plane, with associate mineral microstructures and repartition of the different shell sac cell types. The pillar distribution (*i.e.* vertical alignment and being closer near chamber openings) has been drawn respectively with our observations and previously made descriptions. Note that around 100 chambers traditionally constitute an adult *S. officinalis* shell. For convenience, only three chambers have been drawn here. Arrows indicate the shell sac area where gas and liquid exchanges occur. DS: dorsal shield, CH: chambered part.

Figure 2: Infrared spectra of the acid-insoluble (AIM; A) and acid-soluble (ASM; B) matrices obtained by complete decalcification of the dorsal shield (solid line) and the chambered part (dashed line) from the *Sepia officinalis* shell.

Figure 3: Electrophoretic analysis of the acid-insoluble matrices of the dorsal shield (A) and the chambered part (B) of *S. officinalis* shell. The gels were stained with CBB (lanes 1), silver nitrate (lanes 2), periodic acid Schiff (lanes 3), Alcian blue at pH 2.5 (lanes 4) and pH 1 (lane 5); MM: molecular mass markers. Because of no staining, lane 5 is not presented for B. All bands from these two extracts were excised from the gel for MALDI-TOF/TOF mass spectrometer analyses.

Figure 4: Electrophoretic analysis of the acid-soluble matrices of the dorsal shield (A) and the chambered part (B) of *S. officinalis* shell. The gels were stained with CBB (lanes 1), silver nitrate (lanes 2), periodic acid Schiff (lanes 3) and Alcian blue at pH 2.5 (lanes 4); MM: molecular mass markers. Both matrices were stained with Alcian blue at pH 1 without bands appearance. All bands from these two extracts were excised from the gel for MALDI-TOF/TOF mass spectrometer analyses. Framed band size corresponds to the band allowing protein identification after tryptic digestion and MS analysis.

Figure 5: 2-DE analysis of the acid-insoluble matrices of the dorsal shield (A) and the chambered part (B) of *S. officinalis* shell. The 1-D gels (left) with respective extracts show the correspondence between the protein bands and the spots observed on the 2-D gel (right) after CBB staining.

Figure 6: 2-DE analysis of the acid-soluble matrices of the dorsal shield (A) and the chambered part (B) of *S. officinalis* shell. The 1-D gels (left) with respective extracts show the correspondence between the protein bands and the spots observed on the 2-D gel (right) after CBB staining. Framed band size corresponds to the band allowing protein identification after tryptic digestion and MS analysis.

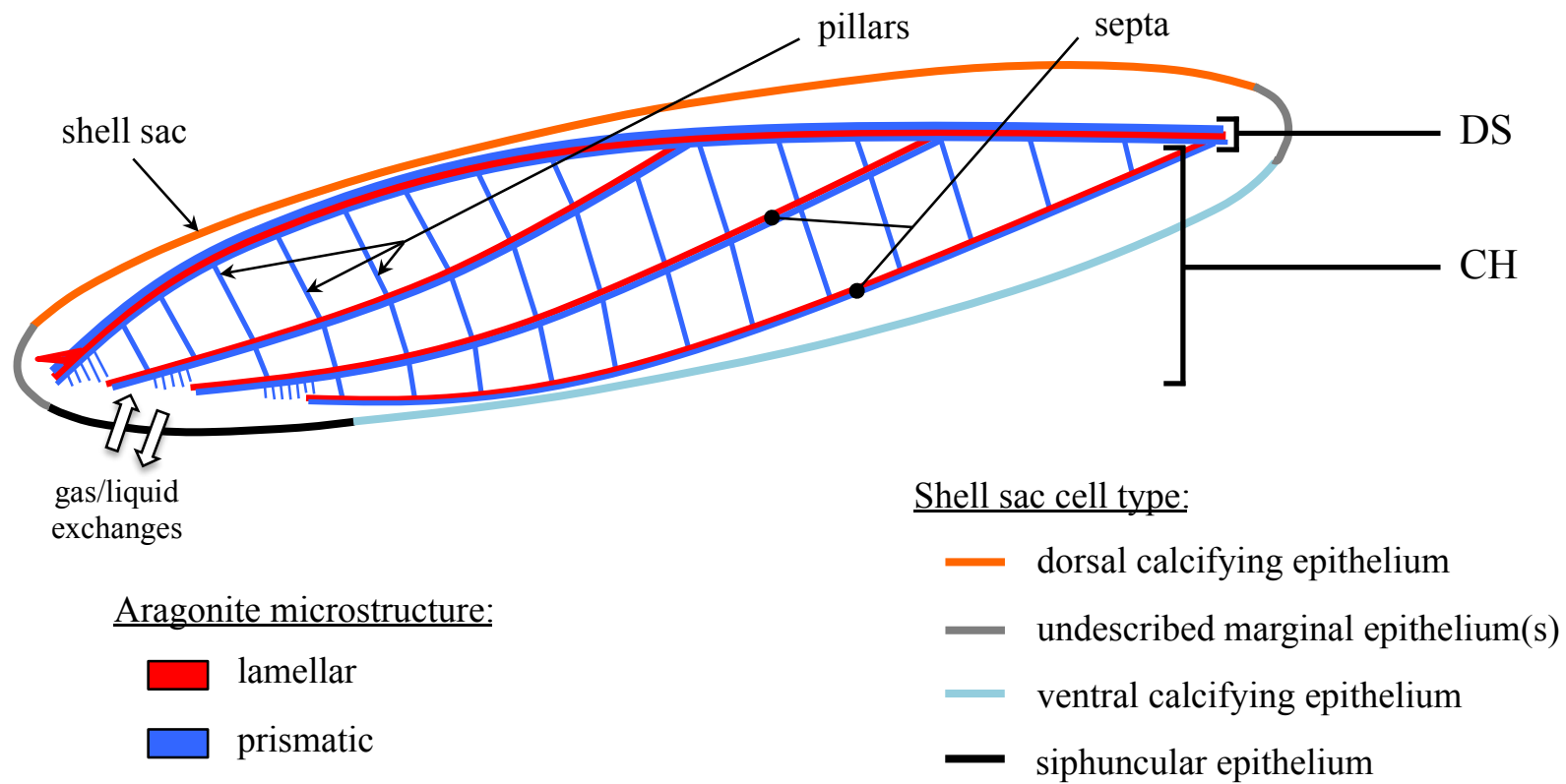


Figure 1

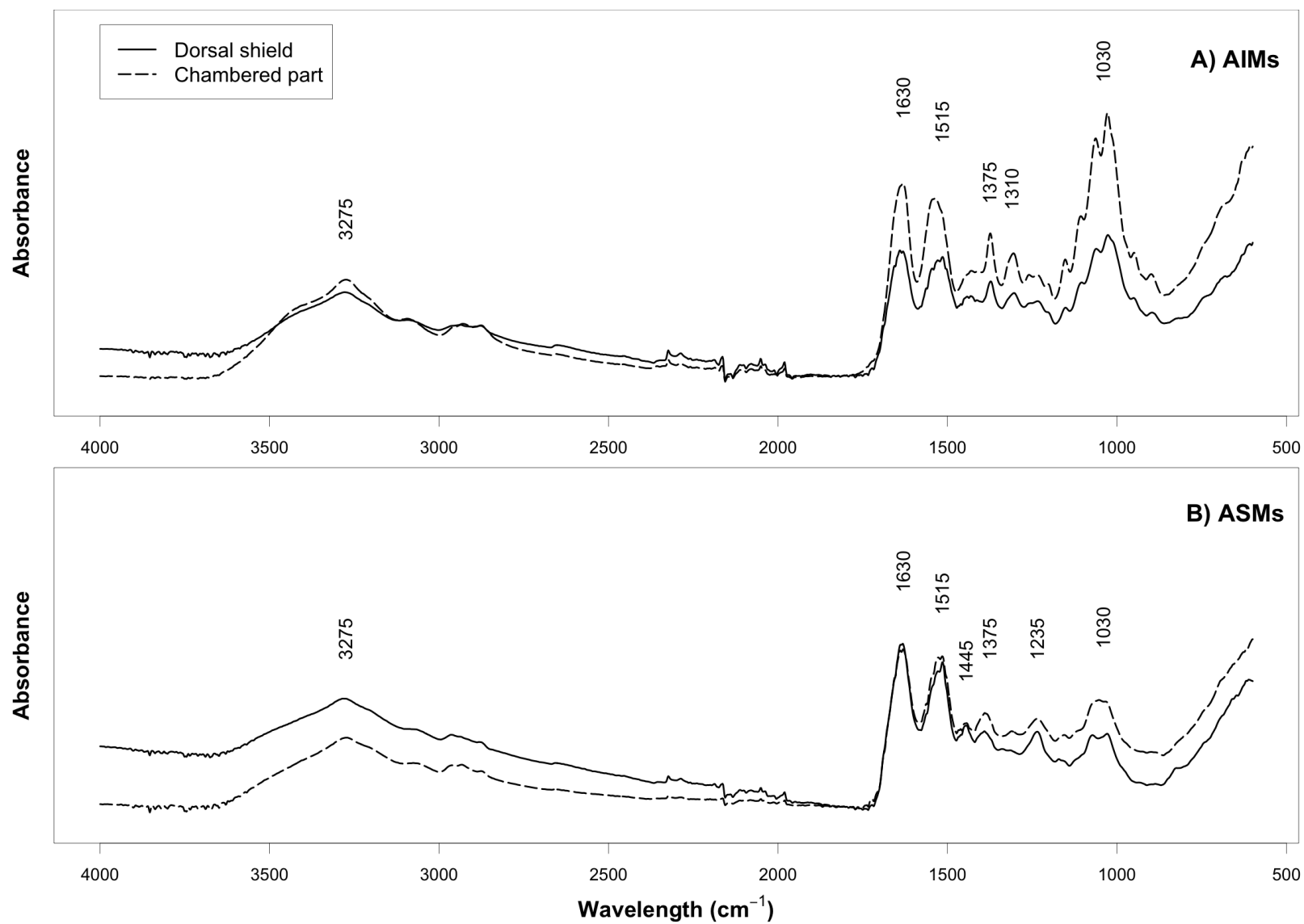
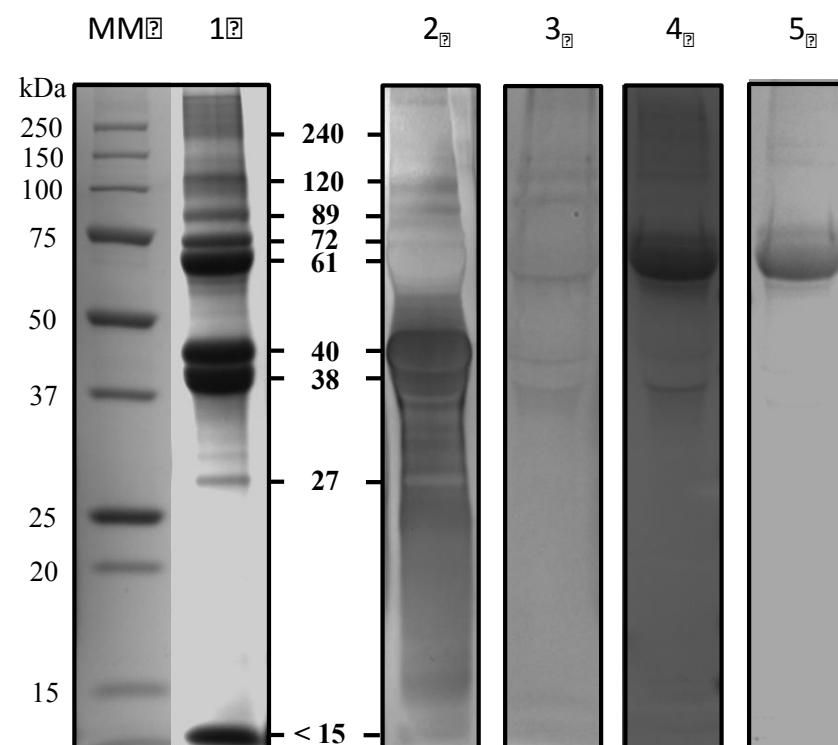


Figure 2

# **A) $\beta$ LS-AIM<sub>DS</sub>**



# **B) $\beta$ LS-AIM<sub>CH</sub>**

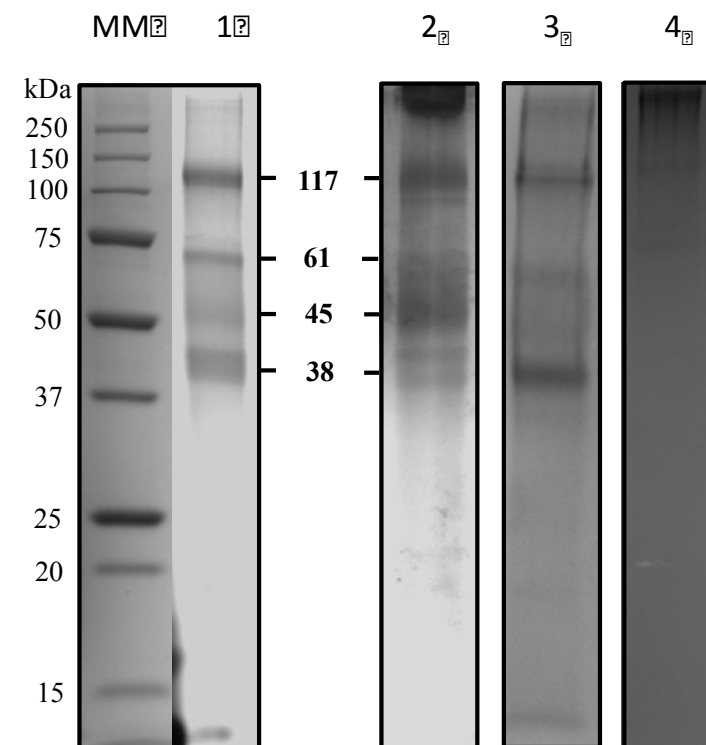
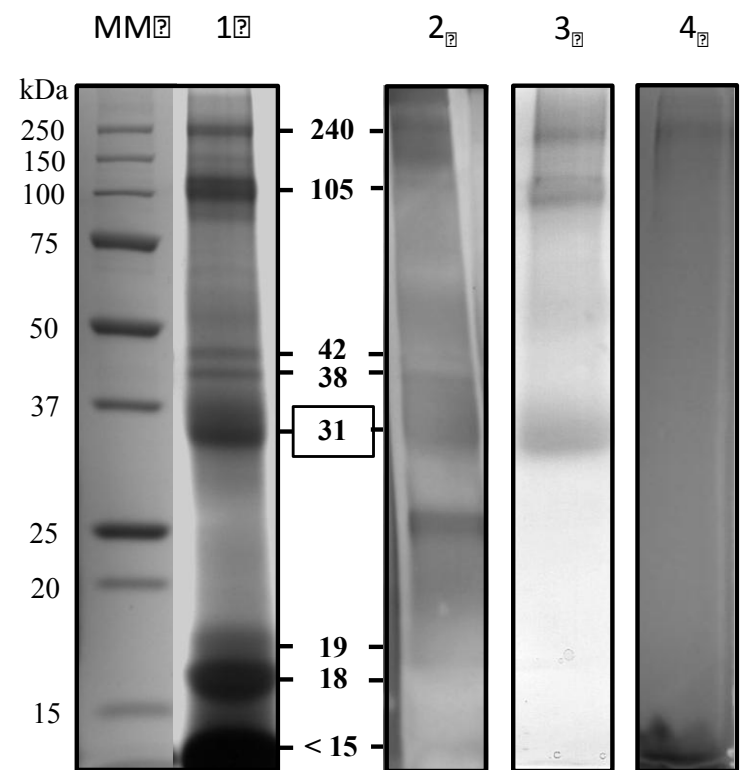


Figure 3

**A) ASM<sub>DS</sub>**



**B) ASM<sub>CH</sub>**

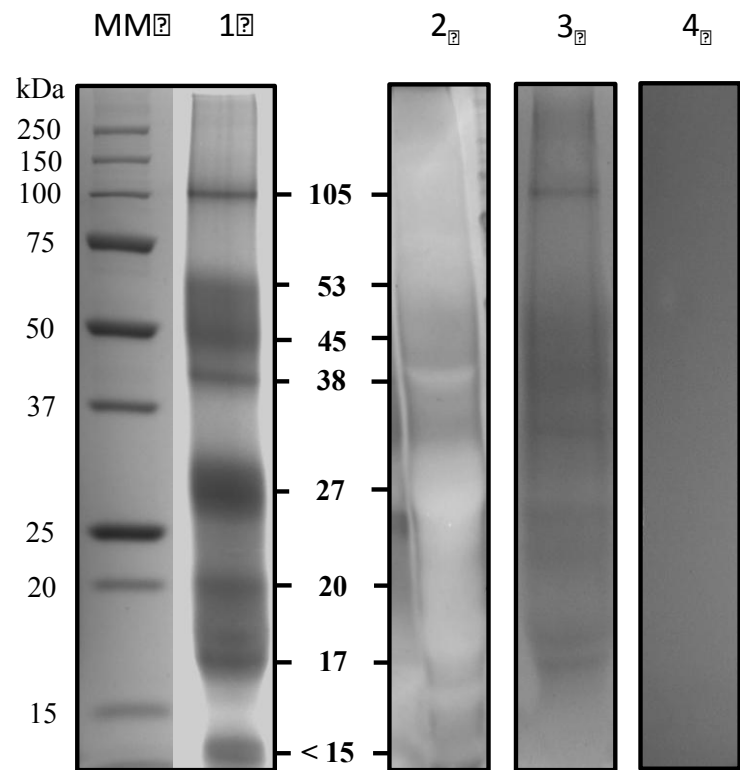


Figure 4



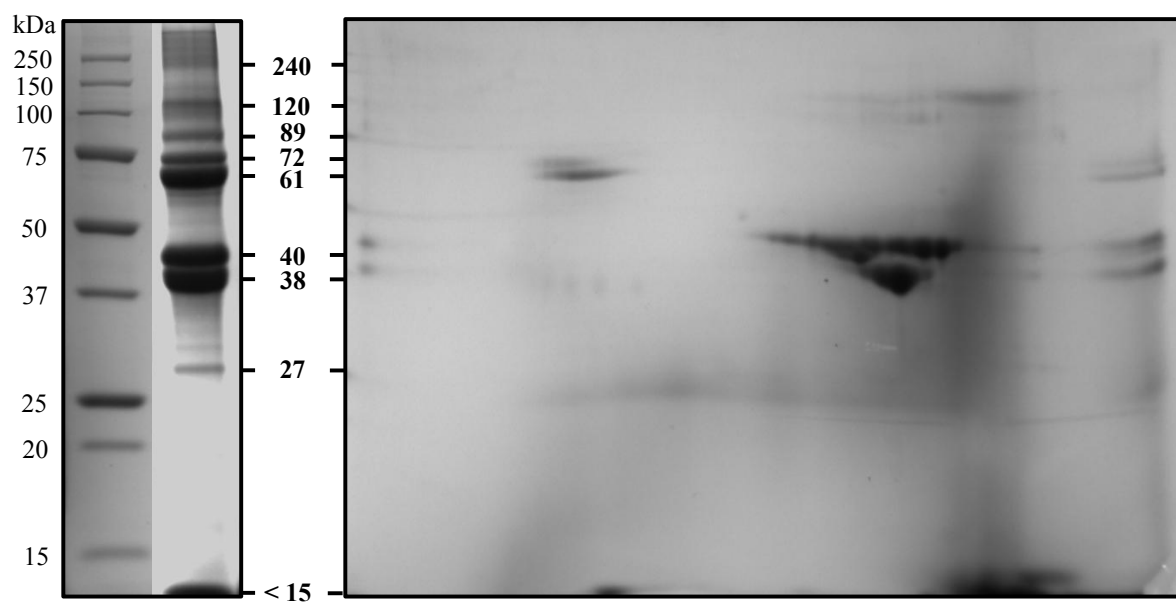
A)  $\text{US-AIM}_{\text{DS}}$

p/□

3?

10?

MM? CBB?



**B)  $\text{US-AIM}_{\text{CH}}$**

p/□

3?

10?

MM? CBB?

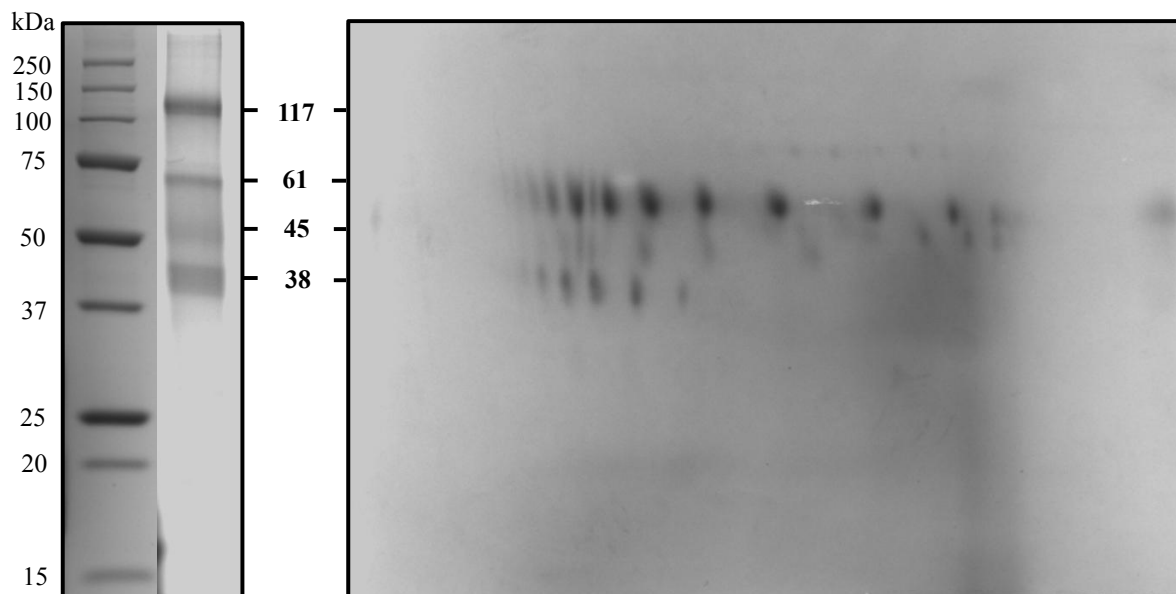


Figure 5

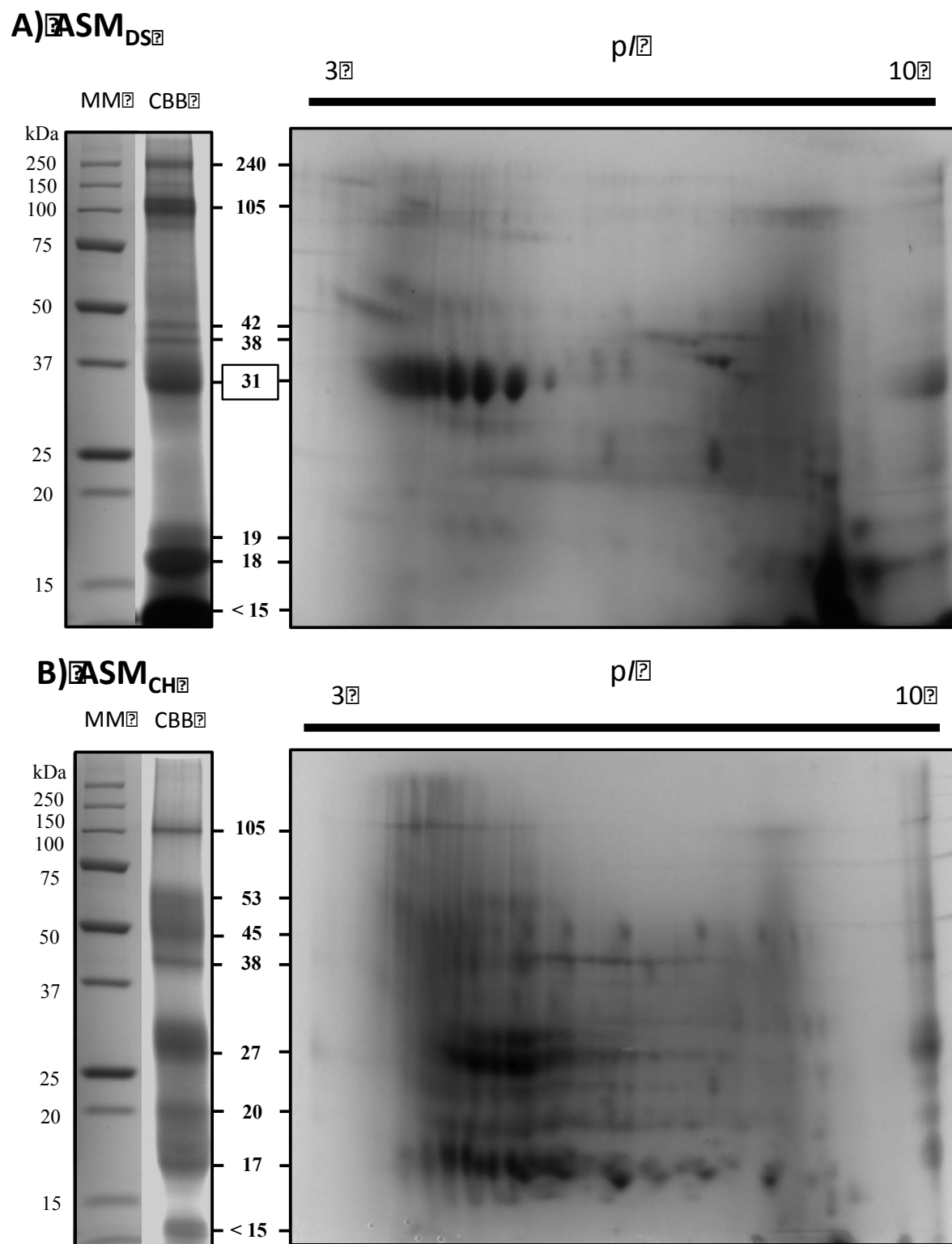


Figure 6

**Supplementary material**  
[Click here to download Supplementary material: Supplementary Table.docx](#)